

DOI:10.1002/ejic.201402071

Use of Organomolybdenum Compounds for Promoted Hydrolysis of Phosphoester Bonds in Aqueous Media

Ana C. Gomes,^[a] Carla A. Gamelas,^[b,c] José A. Fernandes,^[a]
Filipe A. Almeida Paz,^[a] Patrique Nunes,^[d] Martyn Pillinger,^[a]
Isabel S. Gonçalves,^[a] Carlos C. Romão,^[b] and Marta Abrantes*^[d]

Keywords: Indenyl ligands / Molybdenum / Coordination modes / Oxido ligands / Phosphoesters / Hydrolysis

The dissolution of the indenyl (Ind) complex $[(\eta^5\text{-Ind})\text{-Mo}(\text{CO})_2(\mu\text{-Cl})_2]$ (**1**) in *N,N'*-dimethylformamide (DMF) gives the ring-slipped complex $[(\eta^3\text{-Ind})\text{Mo}(\text{CO})_2\text{Cl}(\text{DMF})_2]$ (**2**). The aerial oxidation of **2** leads to the formation of the dinuclear oxomolybdenum(V) chloride $[\text{Mo}_2\text{O}_2(\text{DMF})_4(\mu\text{-O})_2\text{Cl}_2]$ (**3**). The structures of **2** and **3**·DMF have been determined by single-crystal X-ray diffraction. Compounds **1** and **3** were examined as promoters of phosphoester bond hydrolysis in *para*-nitrophenylphosphate (*p*NPP), which was used as a model substrate. The reactions were performed in aqueous solution at 55 °C and followed by ¹H NMR spectroscopy. For assays performed with 30–100 mol-% of **1** or **3** relative to *p*NPP, both compounds promote the production of *para*-nitrophenol (*p*NPh) from *p*NPP. Compound **3** is especially active in promoting the hydrolytic cleavage of the phosphoester bond ($t_{1/2} < 80$ min).

transition metals to phosphoester bond hydrolysis has been studied for a few examples, such as Ti,^[4] V,^[5,6] Mn,^[7–10] Zr,^[11] and Mo,^[12–23] but still remains largely unexplored. Molybdenum is an essential trace element for plant growth, and molybdenum oxides are commonly used as fertilizers to avoid molybdenum deficiencies in soils worldwide;^[24] therefore, molybdenum compounds are interesting candidates for the metal-promoted hydrolysis of phosphoesters. The use of molybdenum compounds as hydrolysis-promoting agents of phosphoesters has been reported with molybdenocene derivatives $[\text{Cp}'_2\text{MoCl}_2]$ (Cp' = substituted cyclopentadienyl),^[12–15] $[\text{MoO}_2\text{Cl}_2\text{L}]$ and $[\text{MoO}_2\text{Me}_2\text{L}]$ complexes (L = no ligand, mono-, or bidentate ligands),^[22,23] molybdates,^[16–20] polyoxometalate derivatives,^[17,21,22] and molybdenum oxide based inorganic–organic hybrids.^[23] The effect of molybdates on phosphoester hydrolysis was originally studied in the context of analytical colorimetric methods for organic phosphate estimation during the 1950s.^[25–27] To study the analytical interferences between organic and inorganic phosphates, these studies were conducted on a wide variety of substrates. More recently, a growing interest in the biological activity of molybdenum compounds and their interactions with phosphate-containing biomolecules has arisen. These studies are typically conducted with model substrates such as *para*-nitrophenylphosphate (*p*NPP),^[12,13,18,22,23] 2-hydroxypropyl-4-nitrophenyl phosphate (HPNP),^[20] phenylphosphate,^[18] bis(*para*-nitrophenyl)phosphate,^[12] and dimethylphosphate.^[15] Reports of studies performed with biological substrates are limited to adenosine triphosphate (ATP).^[16,17,21]

Introduction

Organophosphate pesticides are the most significant cause of severe toxicity and death from acute poisoning worldwide and are responsible for more than 200000 deaths each year in developing countries.^[1,2] Moreover, their accumulation in the environment is a recognized ecological threat and they have harmful effects on human beings and other mammalian species owing to possible long-term exposure to sublethal doses.^[3]

Chemically, organophosphate pesticides are esters of phosphoric acid (phosphoesters). Hydrolysis products of organophosphate pesticides are either nontoxic or have a substantially lower toxicity than the original substrates.^[3] Thus, hydrolysis is considered to be a possible strategy to eliminate organophosphate pesticides. In the absence of a catalyst or enzyme, phosphoester hydrolysis may be extremely slow under normal conditions. For this reason, over time, a growing interest in the metal-promoted hydrolysis of phosphoesters has arisen. The application of group 4–7

[a] Department of Chemistry, CICECO, University of Aveiro, Campus Universitário de Santiago, 3810-193 Aveiro, Portugal

[b] Instituto de Tecnologia Química e Biológica da Universidade Nova de Lisboa, Av. da República, Estação Agronómica Nacional, 2780-157 Oeiras, Portugal

[c] Escola Superior de Tecnologia, Instituto Politécnico de Setúbal, 2910-761 Setúbal, Portugal

[d] Centro de Química Estrutural, Complexo Interdisciplinar, Instituto Superior Técnico, Universidade de Lisboa, 1049-001 Lisbon, Portugal
E-mail: marta.abrantes@ist.utl.pt
http://cqe.ist.utl.pt/pages/marta_abrantes.php

Supporting information for this article is available on the WWW under <http://dx.doi.org/10.1002/ejic.201402071>.

As part of our ongoing work to explore molybdenum complexes for the promoted hydrolysis of phosphoesters, we have now studied the performance of the dimeric chloride complex $[\{(\eta^5\text{-Ind})\text{Mo}(\text{CO})_2(\mu\text{-Cl})\}_2]$ (**1**; Ind = indenyl) as a hydrolysis-promoting agent of *p*NPP in aqueous media. Compound **1** is of interest for this reaction owing to its possession of Cl ligands, which are prone to hydrolysis and substitution by oxygen ligands. Furthermore, indenyl complexes are potentially interesting as catalyst precursors owing to the propensity of this ligand to undergo haptotropic shifts (i.e., ring slippage from η^5 to η^3 hapticity) induced by electrochemical reduction or ligand addition. This haptoflexibility plays an important role in many catalytic processes.^[28–30]

In this study, we further report that the dissolution of **1** in *N,N*-dimethylformamide (DMF) gives the ring-slipped complex $[(\eta^3\text{-Ind})\text{Mo}(\text{CO})_2\text{Cl}(\text{DMF})_2]$ (**2**), which subsequently can undergo aerial oxidation to give the dinuclear oxomolybdenum(V) chloride $[\text{Mo}_2\text{O}_2(\text{DMF})_4(\mu\text{-O})_2\text{Cl}_2]$ (**3**). Compound **3** was also examined as a hydrolysis-promoting agent, and the results are compared with those obtained for $\text{Mo}(\text{CO})_6$ and $[\text{MoO}_2\text{Cl}_2(\text{DMF})_2]$.

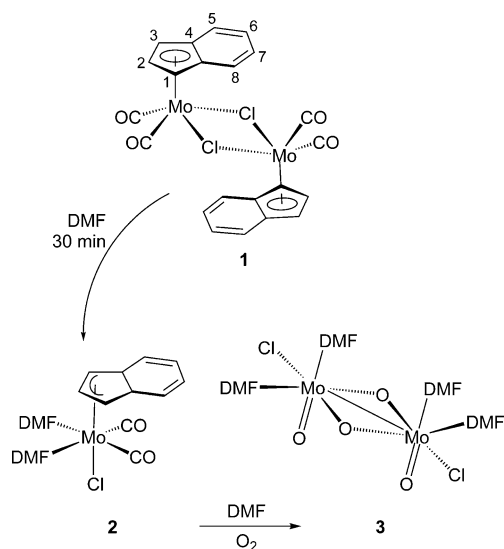
Results and Discussion

Synthesis

The indenyl complex $[\{(\eta^5\text{-Ind})\text{Mo}(\text{CO})_2(\mu\text{-Cl})\}_2]$ (**1**) was synthesized in nearly quantitative yield by the reaction of $[(\eta^5\text{-Ind})\text{Mo}(\eta^3\text{-C}_3\text{H}_5)(\text{CO})_2]$ with HCl (1 M in diethyl ether) in dichloromethane at room temperature. The method is particularly attractive as the allyl precursor is conveniently available from $[\text{Mo}(\eta^3\text{-C}_3\text{H}_5)\text{Cl}(\text{CO})_2(\text{NCMe})_2]$ and KInd in almost quantitative yield.^[31,32] Recently, Honziček et al. isolated dimeric **1** after bubbling gaseous HCl through a solution of $[(\eta^5\text{-Ind})\text{Mo}(\eta^3\text{-C}_3\text{H}_5)(\text{CO})_2]$.^[33] Under similar reaction conditions, bubbling gaseous HCl through the solution at a high flow rate instead of HCl (1 M in diethyl ether) in a more controlled reaction produces $[(\eta^5\text{-Ind})\text{Mo}(\text{CO})_2\text{Cl}_3]$ in excellent yield.^[34] In the solid state, **1** is stable to air and moisture for several hours. The solid-state ^{13}C cross-polarization magic angle spinning (CP MAS) NMR spectrum presents the indenyl signals with chemical shifts characteristic of the η^5 -coordination mode, which are similar to those observed for other η^5 -indenyl ligands such as those in $[(\eta^5\text{-Ind})\text{Mo}\{\kappa^2\text{-S}_2\text{P}(\text{OEt})_2\}(\text{CO})_2]$ ^[35] and $[(\eta^5\text{-Ind})\text{Mo}(\eta^3\text{-C}_3\text{H}_5)(\text{CO})_2]$.^[36]

Compound **1** can be dissolved in DMF to give a brown solution. The color change is due to the immediate formation of $[(\eta^3\text{-Ind})\text{Mo}(\text{CO})_2\text{Cl}(\text{DMF})_2]$ (**2**, Scheme 1). Accordingly, the addition of diethyl ether, pentane, or *n*-hexane to the freshly prepared (30 min) solution results in the immediate precipitation of **2** as a brown solid rather than the dimeric complex **1**. The IR spectrum of **2** shows two strong $\nu(\text{CO})$ absorptions at 1830 and 1934 cm^{-1} (cf. 1851 and 1954 cm^{-1} for **1**) and a very strong band at 1638 cm^{-1} for the carbonyl stretching vibration of the coordinated

DMF molecule. The NMR spectra obtained shortly after dissolving **1** in $[\text{D}_7]\text{DMF}$ show only the presence of **2**. At room temperature, the ^1H NMR spectrum shows rather broad peaks, which suggests that there are extensive dynamic structural interconversions (Figure 1b). The broadening of the signals is even more pronounced at 55 °C (Figure 1a). At –10 °C (Figure 1c), the spectrum becomes well resolved, and sharp resonances are observed for the indenyl protons 1-H and 3-H (doublet), 2-H (triplet), and 5-H/8-H



Scheme 1. Synthesis of **2** and **3** from **1**.

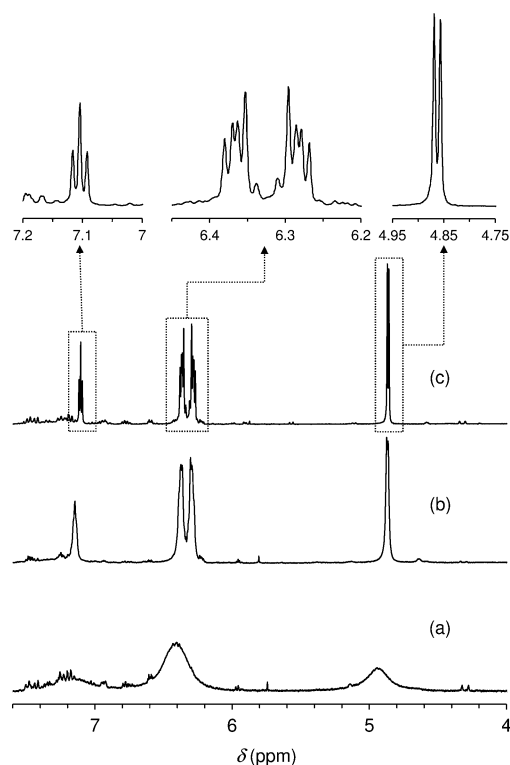


Figure 1. ^1H NMR spectra recorded at (a) 55 °C, (b) room temperature, and (c) –10 °C of the solution obtained after dissolving **1** in $[\text{D}_7]\text{DMF}$.

and 6-H/7-H (two multiplets). The pattern of signals for the indenyl protons is very similar to that found for $[(\eta^3\text{-Ind})\text{Mo}(\text{CO})_2(\text{DMF})_3]\text{BF}_4$.^[37] The η^3 -coordination mode of the indenyl ligand in these complexes is evident mainly from the resonance of the proton in the 2-position. For **2**, this signal appears at lower field ($\delta = 7.10$ ppm) than the signals of the protons of the six-membered ring of the indenyl ligand (5-H to 8-H: $\delta = 6.28, 6.36$ ppm), whereas η^5 -indenyl molybdenum compounds have the signal of 2-H at higher field.^[35]

In a separate experiment, compound **1** was dissolved in DMF, and the solution was layered with pentane and diethyl ether. After storage in a fridge for 3 d under air, red crystals of the known dinuclear oxomolybdenum(V) chloride $[\text{Mo}_2\text{O}_2(\text{DMF})_4(\mu\text{-O})_2\text{Cl}_2]$ (**3**) were obtained (Scheme 1). Compound **3** was previously isolated by Aguado et al. after slow diffusion of diethyl ether into a solution of $[\text{MoO}_2\text{Cl}_2(\text{DMF})_2]$ and PPh_3 in DMF.^[38] The isolation of **3** is in line with a previous report by Sarkar and co-workers in which the aerial oxidation of $[\text{Mo}(\eta^3\text{-C}_3\text{H}_5)\text{Cl}(\text{CO})_2(\text{L})]$ [L = bis(3,5-dimethylpyrazolyl)methane] gave the dimeric oxomolybdenum(V) complex $[\text{Mo}_2\text{O}_2(\text{L})_2(\mu\text{-O})_2\text{Cl}_2]$.^[39] We may conclude that the dissolution of **1** in DMF initially gives **2**, which slowly transforms into **3** in the presence of oxygen. Accordingly, the ^1H NMR spectrum of an aged (4 d) solution of **1** in $[\text{D}_7]\text{DMF}$ showed no signals for the η^5 -indenyl group and the appearance of several weak signals between $\delta = 6.4$ and 7.6 ppm, which may be assigned to indene.

Crystal-Structure Descriptions

Compound **2** crystallizes in the centrosymmetric triclinic space group $P\bar{1}$, and the asymmetric unit is composed of a whole $[(\eta^3\text{-Ind})\text{Mo}(\text{CO})_2\text{Cl}(\text{DMF})_2]$ molecular complex, as depicted in Figure 2. Considering the center of the η^3 -group as a coordination site, the coordination environment around the metal center is best envisaged as a highly distorted octahedron. The $\text{Mo}-\text{C}_{\text{carbonyl}}$ and $\text{Mo}-\text{O}$ distances are in the 1.9383(15)–1.9504(15) Å and 2.2223(10)–

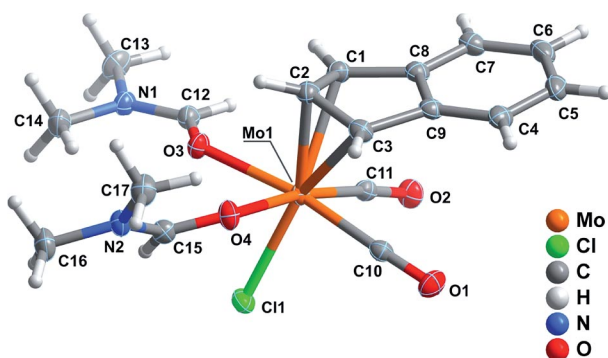


Figure 2. The asymmetric unit of **2**. Non-hydrogen atoms are represented as thermal ellipsoids drawn at the 50% probability level, and hydrogen atoms are represented as small spheres with arbitrary radii. For selected bond lengths and angles of the Mo^{II} coordination sphere, see Table S1.

2.2268(10) Å ranges, respectively, and the unique $\text{Mo}-\text{Cl}$ distance is significantly longer at 2.4747(4) Å (see Figure 2 and Table S1). The *cis* and *trans* octahedral angles are in the 75.91(6)–105.42(5)° and 171.10(5)–173.8° ranges, respectively. The wide distribution of the former angles with respect to the ideal value is attributed to the very distinct nature and steric impediment of the various organic ligands that compose the metal coordination sphere, which ultimately lead to a diversity of angles to minimize mutual steric repulsion.

The hinge angle (HA), fold angle (FA), and $\Delta\text{Mo}-\text{C}$ are important parameters to characterize the coordination mode of the indenyl ligand to the Mo^{II} metal center.^[40,41] For **2**, these parameters were calculated as $\text{HA} = 23.23(16)^\circ$, $\text{FA} = 24.13(15)^\circ$, and $\Delta\text{Mo}-\text{C} = 0.764$ Å and clearly support the η^3 -hapticity of the indenyl ligand. Each pair of neutral CO and DMF ligands is mutually *cis* in the equatorial positions in the coordination octahedron of Mo^{II} . The geometric orientations of the DMF ligands are different from each other, mainly because of distinct supramolecular contacts: one DMF ligand is not engaged in any structurally relevant contacts, whereas the other participates both in $\text{C}-\text{H}\cdots\text{O}$ and in $\text{C}-\text{H}\cdots\pi$ interactions (see Table S1).

A remarkable feature of **2** concerns the unusual metal coordination environment. A search in the literature reveals that only three other monometallic structures of the type $[\text{Cp}'\text{MoL}_n\text{X}]^n$ (Cp' is any substituted cyclopentadienyl, L is any neutral κ^1 ligand, and X is any halogen; no restrictions on the value of n) exist.^[42] Among the compounds of this type, **2** stands out because it is neutral and is the first to have carbonyl or indenyl ligands and η^3 -hapticity for the Cp' ring.

As for **2**, **3** also crystallizes in the centrosymmetric triclinic space group $P\bar{1}$, and the asymmetric unit is composed of a whole dimeric molecular unit formulated as $[\text{Mo}_2\text{O}_2(\text{DMF})_4(\mu\text{-O})_2\text{Cl}_2]$ (see Figure S2). In addition, the asymmetric unit contains a free DMF molecule, which is disordered over two distinct crystallographic sites (rates of occupancy of 0.80:0.20) that share the same position for the nitrogen atom. Complex **3** has already been described by Aguado et al. in a crystal structure without the presence of the solvent molecule of crystallization.^[38] Indeed, the two dimeric $[\text{Mo}_2\text{O}_2(\text{DMF})_4(\mu\text{-O})_2\text{Cl}_2]$ complexes are structurally very similar (see Table S2 for geometrical details of the coordination environments), and small differences only occur in the conformations of the coordinated DMF molecules (to accommodate the disordered solvent molecule of crystallization in the crystal structure). Except for a large number of weak hydrogen-bonding interactions of the type $\text{C}-\text{H}\cdots\text{O}$ and $\text{C}-\text{H}\cdots\text{Cl}$, the crystal structure of **3**·DMF is devoid of noticeable supramolecular interactions (see Table S3).

Crystal packing diagrams for **2** and **3**·DMF are given in the Supporting Information (Figures S1 and S3).

Phosphoester Bond Hydrolysis

Sodium *para*-nitrophenylphosphate (*p*NPP) was used as a model substrate for the phosphoester bond hydrolysis re-

[Mo₂O₂(DMF)₄(μ-O)₂Cl₂] (**3**) is a very efficient hydrolysis promoter with $t_{1/2} < 80$ min (remaining *p*NPP after 80 min of reaction = 37%). Over time, and especially after hydrolysis of 80% of *p*NPP, the reaction rate for the dimeric system clearly slows down, and its profile merges with that for [MoO₂Cl₂(DMF)₂].

These results are interesting in the context of the previously reported data with group 4–7 transition metals. Although comparison of performance with promoters studied in different research groups is very difficult owing to the variability between substrates, reaction conditions, and output measures, some qualitative considerations can still be made.

One important advantage of the system described here is the amount of promoter used (60–200 mol-% of Mo relative to *p*NPP). Previous studies of phosphoester hydrolysis of *p*NPP promoted by group 4–7 transition metals have generally been performed with a large excess of metal in relation to the substrate: between 1.1×10^4 and 3.3×10^5 mol-% of Mo relative to *p*NPP for [Cp'₂Mo(OH)(H₂O)]⁺,^[12,15] between 6.8×10^3 and 3.4×10^4 mol-% of Mo relative to *p*NPP for [(NH₄)₂(MoO₄)],^[27] between 4×10^3 and 6×10^3 mol-% of Ti relative to *p*NPP for titanocene derivatives (Cp'₂TiCl₂),^[4] 1×10^3 mol-% of V relative to *p*NPP for polyoxovanadates ([V₄O₁₂]⁴⁻, [V₅O₁₅]⁵⁻, and [V₁₀O₂₈]⁶⁻),^[5,6] and between 1.4×10^4 and 3.6×10^4 mol-% Mn relative to *p*NPP for MnO₂.^[7] Exceptions, in which the reactions were performed with catalytic or equimolar amounts of metal compound relative to *p*NPP include (1) the reports by Parac-Vogt and co-workers with 70 mol-% of Mo with polyoxomolybdates^[18] and (2) our reports with 10–100 mol-% of Mo with [MoO₂X₂L] derivatives (X = Cl, Me) for the substrate *p*NPP.^[22,23] Very recently, Hupp et al. reported the use of the Zr-based metal–organic framework (MOF) UiO-66 for the hydrolysis of a methylated version of *p*NPP (methyl paraoxon) with an exceptionally low load of accessible metal (0.27 mol-% of Zr) derived from the use of 36 mol-% of Zr relative to methyl paraoxon.^[11]

The best results with molybdenum were obtained for reactions performed with molybdenocenes at 20 °C, which afforded half-times in the same range as that obtained with **3** ($t_{1/2} < 1$ h).^[12,13,15] However, in addition to high Mo/*p*NPP molar ratios (between 1.1×10^4 and 3.3×10^5 mol-% relative to *p*NPP), the molybdenocenes have an imperative requirement for an inert atmosphere (no reaction occurs under air). This inert atmosphere requirement does not exist for all the other reported systems including ours.

To understand the stability and reactivity of **1** and **3** in the reaction medium (water), stability tests were also performed (see Experimental Section for details). After 48 h of stirring **1** in the presence of water at 55 °C for 48 h, a biphasic solid–liquid system was obtained [solid (**1a**), liquid (**1b**)]. The solid **1a** was identified by FTIR spectroscopy as **1** in 70% yield, which indicates that **1** has a low solubility in water (as already detected in the hydrolysis assays) and that the solid is not moisture sensitive. The solution **1b** was analyzed by ESI mass spectrometry. The negative-ion ESI mass spectrum of **1b** exhibits one series of polyoxo-

molybdate anions, namely, [Mo_{*m*}O_{3*m*+1}]²⁻ ($m = 17$ – 22),^[43,44] which indicates that **1** is prone to hydrolysis of the indenyl and Cl ligands and subsequent water condensation reactions. The positive ESI mass spectrum of **1b** exhibits a peak at $m/z = 115$, which is characteristic of [C₉H₇]⁺, a typical metal-free ion in the mass spectra of indenyl derivatives.^[45] In the positive ESI mass spectrum, a mixture of peaks with a characteristic isotopic distribution for monomeric Mo-containing species is also present. Further studies will be needed to unambiguously identify these species.

Phosphoester hydrolysis assays with **3** lead to a monophasic brown system. In addition to peaks for *p*NPP and *p*NPh, the ¹H NMR spectrum of the hydrolysis reaction shows peaks of DMF, which originate from the metal promoter ($\delta = 7.93$, 3.02, and 2.86 ppm). Over time, a new set of singlets appears at $\delta = 8.24$ and 2.72 ppm, which can be assigned to formic acid (FA) and the dimethylammonium (DMA) cation, respectively. The appearance of these peaks had already been reported in our previous work with [MoO₂Cl₂(DMF)₂].^[22] Both [MoO₂Cl₂(DMF)₂] and compound **3** lead to acidic solutions with a pD of 1.41, which can be attributed to the hydrolysis of the Mo–Cl bonds and the formation of HCl. Under these conditions, the degradation of DMF to give FA and DMA ions is likely accelerated. Interestingly, the appearance of the NMR peaks of FA and DMA ions (starting at 44 h) coincides with the slowing down of the reaction. The negative-ion ESI mass spectrum of a solution obtained after stirring **3** with water at 55 °C for 48 h shows, among others, multiple peaks of polymeric Mo-containing species, namely, a series of polyoxomolybdate [Mo_{*m*}O_{3*m*+1}]²⁻ anions ($m = 15$ – 22), similar to **1b**.

Conclusions

We have reported that the dissolution of the dimeric chloride complex [{(η⁵-Ind)Mo(CO)₂(μ-Cl)}₂] (**1**) in DMF gives the ring-slipped complex [(η³-Ind)Mo(CO)₂Cl(DMF)₂] (**2**). The mild aerial oxidation of **2** leads to the dinuclear oxomolybdenum(V) chloride [Mo₂O₂(DMF)₄(μ-O)₂Cl₂] (**3**). Complexes **1** and **3** can be used directly as precursors to hydrolytically active species for the phosphoester bond cleavage of *para*-nitrophenylphosphate in aqueous solution to give inorganic phosphate and *para*-nitrophenol as the products of hydrolysis. The mechanism and the scope of this reaction are being investigated in detail (for example, with other substrates such as toxic organophosphate esters) and will be reported in due course. The behavior of **1** upon dissolution in other solvents is also being further investigated.

Experimental Section

Materials and Methods

Microanalyses (CHN) were obtained with a Truspec instrument at the University of Aveiro by M. Marques, and the Mo contents were determined by inductively coupled plasma optical emission

spectroscopy (ICP-OES) at C.A.C.T.I., University of Vigo, Spain. FTIR and FTIR (ATR) spectra were recorded with a Bruker Tensor 27 spectrophotometer in the 350–4000 cm^{-1} range with 256 scans and 4 cm^{-1} resolution. FT-Raman spectra were recorded with a Bruker RFS 100 spectrometer with a Nd:YAG coherent laser ($\lambda = 1064 \text{ nm}$). ^1H , $^{13}\text{C}\{^1\text{H}\}$, $^1\text{H}-^1\text{H}$ COSY and $^1\text{H}-^{13}\text{C}$ heteronuclear multiple quantum coherence (HMQC) NMR spectra were recorded with Bruker Avance II+ 300 and 400 MHz (UltraShieldTM Magnet) spectrometers. Solid-state magic angle spinning (MAS) ^{13}C NMR spectra were recorded at 100 MHz with a Bruker Avance 400 spectrometer with 3 μs ^1H 90° pulses, 2 ms contact time, a spinning rate of 10 kHz, and 3 s recycle delays. Chemical shifts are quoted in parts per million from tetramethylsilane. Electrospray ionization (ESI) mass spectra were obtained with a 500-MS quadrupole ion trap mass spectrometer (Varian Inc., Palo Alto, CA, USA). Samples were introduced into the ESI ion source by using a syringe pump set to a flow rate of 20 $\mu\text{L}/\text{min}$. The ion spray voltage was set at $\pm 5 \text{ kV}$, the capillary voltage was 60–80 V, and the radio frequency (RF) loading was 80%. Nitrogen was used as the nebulizing and drying gas at pressures of 35 and 10 psi, respectively; the drying gas temperature was 350 °C. The spectra were recorded in the range 100–1000 Da. The spectra typically correspond to the average of 20–35 scans. The samples were dissolved in Millipore deionized water immediately prior to the analysis.

Air-sensitive operations were performed by standard Schlenk techniques under a nitrogen atmosphere. Solvents were dried by standard procedures [tetrahydrofuran (THF), diethyl ether, and *n*-hexane over Na/benzophenone ketyl; dichloromethane over CaH_2] and distilled under nitrogen. 1 M HCl in diethyl ether (Sigma–Aldrich), *N,N'*-dimethylformamide (DMF, 99%, Sigma–Aldrich), pentane (99%, Sigma–Aldrich), *n*-hexane (99%, Sigma–Aldrich), D_2O (99.9%, Euroisotop), $[\text{D}_7]\text{DMF}$ (99.5%, Sigma–Aldrich), and 4-nitrophenyl phosphate disodium salt hexahydrate (*p*NPP, 98%, Alfa Aesar) were purchased from commercial sources and used as received. $[(\eta^5\text{-Ind})\text{Mo}(\eta^3\text{-C}_3\text{H}_5)(\text{CO})_2]$ was prepared as previously reported.^[31b]

$[(\eta^5\text{-Ind})\text{Mo}(\text{CO})_2(\mu\text{-Cl})_2]$ (1): HCl (1 M) in diethyl ether (6.0 mL, 6.00 mmol) was added dropwise to a solution of $[(\eta^5\text{-Ind})\text{Mo}(\eta^3\text{-C}_3\text{H}_5)(\text{CO})_2]$ (0.51 g, 1.67 mmol) in CH_2Cl_2 , and the reaction mixture was stirred for 2 h at room temperature. The resultant red brown precipitate was collected by filtration, washed with diethyl ether, and vacuum dried. Yield: 0.49 g (98%). $\text{C}_{22}\text{H}_{14}\text{Cl}_2\text{Mo}_2\text{O}_4$ (605.13): calcd. C 43.66, H 2.33, Mo 31.71; found C 43.39, H 2.32, Mo 32.09. FTIR (KBr): $\tilde{\nu} = 3097$ (w), 2056 (w), 1961 [vs, $\nu(\text{CO})$], 1862 [vs, $\nu(\text{CO})$], 1602 (w), 1542 (m), 1479 (m), 1446 (m), 1376 (m), 1330 (m), 1240 (w), 1220 (w), 1153 (w), 1099 (w), 1037 (m), 984 (m), 902 (m), 829 (s), 745 (vs), 601 (m), 592 (m), 561 (m), 517 (m), 496 (m), 470 (w), 453 (m), 443 (s), 387 (w) cm^{-1} . FT-Raman: $\tilde{\nu} = 3095$ (w), 3070 (w), 3049 (w), 1951 (w), 1842 (m), 1545 (w), 1447 (w), 1376 (w), 1328 (vs), 1240 (w), 1160 (w), 1038 (w), 1006 (w), 908 (w), 738 (w), 594 (w), 562 (w), 520 (w), 496 (m), 458 (w), 390 (m), 284 (m), 262 (w), 184 (w), 165 (s), 122 (vs), 106 (vs) cm^{-1} . ^{13}C CP MAS NMR: $\delta = 265.7$ (CO), 259.2 (CO), 130.2 (C-8, C-9), 129.0 (C-5, C-6), 123.9 (C-4, C-7), 89.9 (C-2), 76.4 (C-1, C-3) ppm.

The NMR spectroscopic data for a freshly prepared solution of **1** in $[\text{D}_7]\text{DMF}$ showed only the presence of $[(\eta^5\text{-Ind})\text{Mo}(\text{CO})_2\text{-Cl}(\text{DMF})_2]$ (**2**). ^1H NMR (300 MHz, $[\text{D}_7]\text{DMF}$, 263 K): $\delta = 7.10$ (t, $J = 6.2 \text{ Hz}$, 1 H, 2-H), 6.36 (m, 2 H, 5-H, 8-H/6-H, 7-H), 6.28 (m, 2 H, 5-H, 8-H/6-H, 7-H), 4.86 (d, $J = 6.2 \text{ Hz}$, 2 H, 1-H, 3-H) ppm. $^{13}\text{C}\{^1\text{H}\}$ (126 MHz, $[\text{D}_7]\text{DMF}$, 263 K): $\delta = 232.7$ (CO), 148.3 (C-4, C-9), 123.8 (C-5, C-8/C-6, C-7), 117.2 (C-5, C-8/C-6, C-7), 103.4 (C-2), 72.5 (C-1, C-3) ppm. $^{13}\text{C},^1\text{H}$ HSQC (126/300 MHz,

$[\text{D}_7]\text{DMF}$, 263 K): $\delta^{13}\text{C}/\delta^1\text{H} = 123.8/6.28$ (C-5, C-8/C-6, C-7), 117.2/6.36 (C-5, C-8/C-6, C-7), 104.4/7.10 (C-2), 73.5/4.86 (C-1, C-3) ppm.

$[(\eta^3\text{-Ind})\text{Mo}(\text{CO})_2\text{Cl}(\text{DMF})_2]$ (2): Compound **1** (0.1 g, 0.17 mmol) was dissolved in DMF (5 mL), and the solution was stirred for 30 min at room temperature under nitrogen. To the brown solution, a layer of diethyl ether was added (10 mL), followed by pentane (30 mL) and *n*-hexane (30 mL). After 10 min, the colorless solution was filtered, and the brown residue was washed with pentane ($3 \times 20 \text{ mL}$) and vacuum-dried. Yield: 0.14 g (90%). $\text{C}_{17}\text{H}_{21}\text{ClMoN}_2\text{O}_4$ (448.75): calcd. C 45.50, H 4.72, N 6.24; found C 44.98, H 4.41, N 5.90. FTIR (ATR): $\tilde{\nu} = 2935$ (w), 1934 [vs, $\nu(\text{CO})$], 1830 [vs, $\nu(\text{CO})$], 1638 (vs), 1494 (w), 1432 (m), 1421 (m), 1378 (m), 1365 (s), 1310 (w), 1250 (w), 1150 (w), 1113 (m), 1060 (w), 1047 (m), 1014 (w), 965 (m), 915 (w), 885 (w), 778 (m), 747 (m), 687 (s), 579 (m), 551 (w), 506 (m), 393 (s), 370 (s) cm^{-1} . ^1H NMR (300 MHz, $[\text{D}_7]\text{DMF}$, 263 K): $\delta = 8.02$ (s, CH), 7.10 (t, $J = 6.2 \text{ Hz}$, 1 H, 2-H), 6.36 (m, 2 H, 5-H, 8-H/6-H, 7-H), 6.28 (m, 2 H, 5-H, 8-H/6-H, 7-H), 4.86 (d, $J = 6.2 \text{ Hz}$, 2 H, 1-H, 3-H), 2.95 (s, CH_3), 2.78 (s, CH_3) ppm. Orange crystals of **2** suitable for X-ray diffraction were obtained by slow diffusion of diethyl ether into a solution of **1** in DMF under nitrogen.

$[\text{Mo}_2\text{O}_2(\text{DMF})_4(\mu\text{-O})_2\text{Cl}_2]$ (3): Compound **1** (0.08 g, 0.13 mmol) was dissolved in DMF (10 mL), and to this solution was added a pentane (20 mL) layer followed by another layer of diethyl ether (20 mL). The solution was kept in a fridge for 3 d under air; this resulted in the formation of red crystals, which were identified as **3**. Yield: 0.05 g, 60%. $\text{C}_{12}\text{H}_{28}\text{Cl}_2\text{Mo}_2\text{N}_4\text{O}_8$ (619.16): calcd. C 23.28, H 4.56, N 9.05; found C 22.96, H 4.68, N 8.85. FTIR (ATR): $\tilde{\nu} = 2939$ (w), 1632 (vs), 1439 (w), 1438 (m), 1366 (m), 1357 (m), 1250 (m), 1157 (w), 1122 (w), 1062 (w), 958 (vs), 940 (m), 868 (w), 802 (w), 741 (m), 721 (m), 699 (m), 684 (s), 498 (m), 490 (m), 470 (m), 384 (vs) cm^{-1} . FT-Raman: $\tilde{\nu} = 2939$ (w), 1546 (m), 959 (m), 787 (vs), 446 (w), 215 (m) cm^{-1} . ^1H NMR (300 MHz, $[\text{D}_7]\text{DMF}$, 263 K): $\delta = 8.01$ (s), 2.94 (s, CH_3), 2.77 (s, CH_3) ppm.

Single-Crystal X-ray Diffraction

Single crystals of compounds **2** and **3**-DMF were manually harvested from the crystallization vials and immediately immersed in highly viscous FOMBLIN Y perfluoropolyether vacuum oil (LVAC 140/13, Sigma–Aldrich) to avoid degradation caused by the evaporation of the solvent.^[46] The crystals were mounted on Hampton Research CryoLoops with the help of a Stemi 2000 stereomicroscope equipped with Carl Zeiss lenses. The data were collected with a Bruker X8 Kappa APEX II CCD area-detector diffractometer (Mo- K_α graphite-monochromated radiation, $\lambda = 0.71073 \text{ \AA}$) controlled by the APEX2 software package^[47] and equipped with an Oxford Cryosystems Series 700 cryostream monitored remotely by using the software interface Cryopad.^[48] Images were processed with SAINT+^[49] and the data were corrected for absorption by the multiscan semi-empirical method implemented in SADABS.^[50] The structures were solved by using the Patterson synthesis algorithm implemented in SHELXS-97,^[51] which allowed the immediate location of the crystallographically independent Mo^{II} or Mo^{V} centers and most of the heaviest atoms. The remaining non-hydrogen atoms were located from difference Fourier maps calculated from successive full-matrix least-squares refinement cycles on F^2 by SHELXL-97.^[51b,52] The DMF molecule of crystallization in **3**-DMF was disordered over two distinct crystallographic positions with an occupancy ratio of 0.8:0.2. The two disordered components were refined with isotropic displacement parameters for the non-hydrogen atoms, and the N–C, C–O, and C···C distances were restrained to be similar by using the SHELXL command SADI. Ad-

ditionally, the central nitrogen atoms were found to be very close and, therefore, were set to be coincident. All non-hydrogen atoms composing the dimetallic neutral cluster were successfully refined with anisotropic displacement parameters.

Most of the hydrogen atoms bound to carbon atoms were placed at their idealized positions by using appropriate HFIX instructions in SHELXL: 33 for the $-\text{CH}_3$ methyl group and 43 for the CH groups of the aromatic rings and the N-CH-O groups. The hydrogen atoms bound to the carbon atoms of the C_5 ring of the indenyl ligand in **2** appeared to adopt inaccurate positions when the HFIX 43 command was used. Therefore, the positions of these atoms were refined with C-H distances restrained to 0.95(1) Å. When the HFIX instruction 33 was used for atom C-9 of **3**·DMF, a large electron density near the carbon atom remained unassigned. Therefore, the HFIX 123 command (corresponding to two pairs of hydrogen atoms with a mutual displacement of 60° and occupancies equal to 0.5) was used instead. All hydrogen atoms were included in subsequent refinement cycles with isotropic thermal displacement parameters (U_{iso}) fixed at $1.2 \times U_{\text{eq}}$ (CH groups) or $1.5 \times U_{\text{eq}}$ (methyl groups) of the parent carbon atoms.

The last difference Fourier map synthesis showed for **2** that the highest peak ($0.402 \text{ e}\text{Å}^{-3}$) was located at 0.73 Å from C9 (center of the indenyl ligand) and the deepest hole ($-0.439 \text{ e}\text{Å}^{-3}$) at 0.70 Å from Mo1; for **3**·DMF the corresponding peak ($0.464 \text{ e}\text{Å}^{-3}$) and hole ($-0.525 \text{ e}\text{Å}^{-3}$) were found at 1.79 Å from C18 and 1.11 Å from Mo1, respectively. Information concerning the crystallographic data collection and structure refinement details is summarized in Table 1. The most relevant geometrical parameters of the molybdenum coordination environments and of the supramolecular con-

tacts in **2** and **3**·DMF are summarized in Tables S1–S3 (Supporting Information).

CCDC-963360 (for **2**) and -963361 (for **3**·DMF) contain the supplementary crystallographic data for this paper. These data can be obtained free of charge from The Cambridge Crystallographic Data Centre via www.ccdc.cam.ac.uk/data_request/cif.

Hydrolysis Reactions: Sodium *para*-nitrophenylphosphate (*p*NPP, 4.0 mg, 0.01 mmol) and dioxane (internal standard, 1.2 mg, 0.013 mmol) were dissolved in deuterated water in a 5 mm NMR tube containing a magnetic stirring bar and heated to 55 °C. The molybdenum compound (variable amounts in the range 30–100 mol-% relative to *p*NPP) was added, and the progression of the reaction was monitored over time by ^1H NMR spectroscopy. *Attention:* The magnetic stirring bar was removed immediately before the NMR measurement, and then reintroduced immediately after the measurement. The relative amounts of *p*NPP and *para*-nitrophenol (*p*NPh) in the reaction medium were followed by quantification of the respective areas in comparison to the area of the internal standard. The pH of the solution was measured at the described reaction temperature. The pD value of the solution was obtained by adding 0.41 to the pH reading. Before the addition of the catalyst, the reaction medium had a pD of 7.4. The addition of the metal complexes studied caused significant differences in the pD of the reaction medium. The reactions were not buffered so that the real impact of each compound per se in the hydrolysis reaction could be understood. The authors are aware that the pD may influence the performance of the systems and that it is difficult to distinguish between the effect of pH and the effect of metal promoter. However, we would like to recall that it is the behavior

Table 1. Crystal data and structure refinement details.

Compound	2	3 ·DMF
Formula	$\text{C}_{17}\text{H}_{21}\text{ClMoN}_2\text{O}_4$	$\text{C}_{12}\text{H}_{28}\text{Cl}_2\text{Mo}_2\text{N}_4\text{O}_8 \cdot \text{C}_3\text{H}_7\text{NO}$
<i>M</i>	448.75	692.26
Temperature/K	150(2)	180(2)
Crystal system	triclinic	triclinic
Space group	$P\bar{1}$	$P\bar{1}$
<i>a</i> /Å	8.6448(6)	9.6781(14)
<i>b</i> /Å	10.7816(9)	11.0819(15)
<i>c</i> /Å	11.4577(9)	14.128(2)
<i>a</i> /°	71.368(3)	85.079(9)
<i>b</i> /°	72.342(2)	75.962(9)
<i>γ</i> /°	77.423(3)	69.251(9)
Volume/Å ³	955.59(13)	1374.7(3)
<i>Z</i>	2	2
$D_{\text{calcd.}}/\text{g cm}^{-3}$	1.560	1.672
$\mu(\text{Mo-K}\alpha)/\text{mm}^{-1}$	0.849	1.155
Crystal size/mm	0.11 × 0.06 × 0.02	0.10 × 0.08 × 0.06
Crystal type	red plate	orange block
θ range /°	1.94–29.26	3.32–25.35
Index ranges	–11 ≤ <i>h</i> ≤ 11 –14 ≤ <i>k</i> ≤ 14 –14 ≤ <i>l</i> ≤ 15	–11 ≤ <i>h</i> ≤ 11 –13 ≤ <i>k</i> ≤ 13 –17 ≤ <i>l</i> ≤ 17
Reflections collected	19118	25419
Independent reflections	5139 [$R_{\text{int}} = 0.0235$]	5033 [$R_{\text{int}} = 0.0678$]
Data completeness	98.8% (to $\theta = 29.26^\circ$)	99.7% (to $\theta = 25.35^\circ$)
Final <i>R</i> indices [$I > 2\sigma(I)$] ^[a,b]	$R_1 = 0.0207$ $wR_2 = 0.0469$	$R_1 = 0.0385$ $wR_2 = 0.0699$
Final <i>R</i> indices (all data) ^[a,b]	$R_1 = 0.0249$ $wR_2 = 0.0484$	$R_1 = 0.0656$ $wR_2 = 0.0799$
Weighting scheme ^[c]	$m = 0.0199$ $n = 0.2981$	$m = 0.276$ $n = 0.7390$
Largest diff. peak and hole/ $\text{e}\text{Å}^{-3}$	0.402, –0.439	0.464, –0.525

[a] $R_1 = \sum |F_o| - |F_c| / \sum |F_o|$. [b] $wR_2 = \{\sum [w(F_o^2 - F_c^2)^2] / \sum [w(F_o^2)^2]\}^{1/2}$. [c] $w = 1 / [\sigma^2(F_o^2) + (mP)^2 + nP]$, where $P = (F_o^2 + 2F_c^2) / 3$.

of the metal promoter in deuterated water that defines the pD of the system and that buffering the system would “mask” this reactivity and, thus, the possible availability of species in solution. The blank reaction was performed without molybdenum compound.

Stability Test for 1: Compound **1** (0.25 g, 0.41 mmol) and H₂O (35 mL) were added to a Schlenk tube. The resultant suspension was stirred at 55 °C for 48 h. The brown precipitate was isolated, washed with water, and vacuum dried to afford the solid **1a**. The remaining pale orange filtrate was designated as **1b**. The solid **1a** was characterized by FTIR spectroscopy and identified as [(η⁵-Ind)Mo(CO)₂(μ-Cl)]₂ (**1**). Yield: 0.18 g (70%). The filtrate **1b** was analyzed by ESI-MS.

Stability Test for 3: Compound **3** (0.6 g, 0.9 mmol) was deaerated, and H₂O (10 mL) was added. The resultant solution was stirred for 48 h at 55 °C to afford the solution **3a**, which was analyzed by ESI-MS.

Supporting Information (see footnote on the first page of this article): Tables of selected bond lengths and angles for **2** and **3**, geometrical details of supramolecular contacts, crystal packing diagrams for **2** and **3**, the molecular structure of **3**.

Acknowledgments

This work was partly financed by FEDER (Fundo Europeu de Desenvolvimento Regional) through COMPETE (Programa Operacional Factores de Competitividade) and by national funds through the FCT (Fundação para a Ciência e a Tecnologia) with the projects CICECO (Centre for Research in Ceramics and Composite Materials) – FCOMP-01-0124-FEDER-037271 (FCT ref. PEst-C/CTM/LA0011/2013), FCOMP-01-0124-FEDER-029779 (FCT ref. PTDC/QEQ-SUP/1906/2012, including the research grant with ref. BPD/UI89/4864/2013 to A. C. G.) – and the Centro de Química Estrutural (PEst-OE/QUI/UI0100/2013). We further wish to thank the FCT for specific funding towards the purchase of the single-crystal diffractometer and for the postdoctoral grant SFRH/BPD/63736/2009 (to J. A. F.). The authors are grateful to M. C. Oliveira for the ESI-MS analysis. The NMR spectrometers are part of The National NMR Network (REDE/1517/RMN/2005), supported by POCI 2010 (Programa Operacional Ciência e Inovação 2010) and the FCT. The authors also thank the Portuguese NMR Network (Instituto Superior Técnico Center) (RECI/QEQ-QIN/0189/2012) for providing access to the NMR facilities.

- [1] S. V. Kumar, M. Fareedullah, Y. Sudhakar, B. Venkateswarlu, E. A. Kumar, *Archiv. Appl. Sci. Res.* **2010**, *2*, 199–215.
- [2] M. Eddleston, N. A. Buckley, P. Eyer, A. H. Dawson, *Lancet* **2008**, *371*, 597–607.
- [3] M. Sirotkina, I. Lyagin, E. Efremenko, *Int. Biodeterior. Biodegrad.* **2012**, *68*, 18–23.
- [4] A. Erxleben, J. Claffey, M. Tacke, *J. Inorg. Biochem.* **2010**, *104*, 390–396.
- [5] N. Steens, A. M. Ramadan, T. N. Parac-Vogt, *Chem. Commun.* **2009**, 965–967.
- [6] N. Steens, A. M. Ramadan, G. Absillis, T. N. Parac-Vogt, *Dalton Trans.* **2010**, *39*, 585–592.
- [7] D. S. Baldwin, D. R. Jones, L. M. Coleman, J. K. Beattie, *Environ. Sci. Technol.* **2001**, *35*, 713–716.
- [8] X. Jia-Qing, C. Yong, L. Ci, Z. Jiu-Jin, H. Wei, Z. Xian-Cheng, *J. Dispersion Sci. Technol.* **2005**, *26*, 693–699.
- [9] W. Jiang, B. Xu, Q. Lin, J. Li, F. Liu, X. Zang, H. Chen, *Colloids Surf. A* **2008**, *315*, 103–109.
- [10] W. D. Jiang, B. Xu, J. Z. Li, J. Q. Xie, H. Y. Fu, H. Chen, X. C. Zeng, *J. Dispersion Sci. Technol.* **2006**, *27*, 869–877.
- [11] M. J. Katz, J. E. Mondloch, R. K. Totten, J. K. Park, S. T. Nguyen, O. K. Farha, J. T. Hupp, *Angew. Chem. Int. Ed.* **2014**, *53*, 497–501; *Angew. Chem.* **2014**, *126*, 507–511.
- [12] M. J. Kuo, S. Kuhn, D. Ly, *Inorg. Chem.* **1995**, *34*, 5341–5345.
- [13] L. Y. Kuo, L. A. Barnes, *Inorg. Chem.* **1999**, *38*, 814–817.
- [14] L. Y. Kuo, N. M. Perera, *Inorg. Chem.* **2000**, *39*, 2103–2106.
- [15] T. J. Ahmed, L. N. Zakharov, D. R. Tyler, *Organometallics* **2007**, *26*, 5179–5187.
- [16] E. Ishikawa, T. Yamase, *J. Inorg. Biochem.* **2006**, *100*, 344–350.
- [17] E. Cartuyvels, K. V. Hecke, L. V. Meervelt, C. Görrler-Walrand, T. N. Parac-Vogt, *J. Inorg. Biochem.* **2008**, *102*, 1589–1598.
- [18] E. Cartuyvels, G. Absillis, T. N. Parac-Vogt, *Chem. Commun.* **2008**, 85–87.
- [19] G. Absillis, R. V. Deun, T. N. Parac-Vogt, *Inorg. Chem.* **2011**, *50*, 11552–11560.
- [20] G. Absillis, E. Cartuyvels, R. V. Deun, T. N. Parac-Vogt, *J. Am. Chem. Soc.* **2008**, *130*, 17400–17408.
- [21] E. Ishikawa, T. Yamase, *Eur. J. Inorg. Chem.* **2013**, 1917.
- [22] C. Tomé, M. C. Oliveira, M. Pillinger, I. S. Gonçalves, M. Abrantes, *Dalton Trans.* **2013**, *42*, 3901–3907.
- [23] A. C. Gomes, M. Pillinger, P. Nunes, I. S. Gonçalves, M. Abrantes, *J. Organomet. Chem.* **2014**, *760*, 42–47.
- [24] U. C. Gupta (Ed.), *Molybdenum in Agriculture*, Cambridge University Press, Cambridge, **1997**.
- [25] H. Weil-Malherbe, R. H. Green, *Biochem. J.* **1951**, *49*, 286–292.
- [26] H. Weil-Malherbe, *Biochem. J.* **1953**, *55*, 741–745.
- [27] L. Lutwak, J. Sacks, *J. Biol. Chem.* **1953**, *200*, 565–569.
- [28] M. J. Calhorda, C. C. Romão, L. F. Veiros, *Chem. Eur. J.* **2002**, *8*, 868–875.
- [29] C. A. Bradley, I. Keresztes, E. Lobkovsky, P. J. Chirik, *Organometallics* **2006**, *25*, 2080–2089.
- [30] a) S. M. Bruno, C. A. Gamelas, A. C. Gomes, A. A. Valente, M. Pillinger, C. C. Romão, I. S. Gonçalves, *Catal. Commun.* **2012**, *23*, 58–61; b) S. M. Bruno, A. C. Gomes, C. A. Gamelas, M. Abrantes, M. C. Oliveira, A. A. Valente, F. A. Almeida Paz, M. Pillinger, C. C. Romão, I. S. Gonçalves, *New J. Chem.* **2014**, *38*, 3172–3180.
- [31] a) J. R. Ascenso, C. G. Azevedo, I. S. Gonçalves, E. Herdtweck, D. S. Moreno, C. C. Romão, J. Zühlke, *Organometallics* **1994**, *13*, 429–431; b) J. R. Ascenso, C. G. Azevedo, I. S. Gonçalves, E. Herdtweck, D. S. Moreno, M. Pessanha, C. C. Romão, *Organometallics* **1995**, *14*, 3901–3919.
- [32] J. W. Faller, C.-C. Che, M. J. Mattina, A. Jakubowski, *J. Organomet. Chem.* **1973**, *52*, 361–387.
- [33] J. Honzík, J. Vinklár, M. Erben, J. Lodinský, L. Dostál, Z. Padělková, *Organometallics* **2013**, *32*, 3502–3511.
- [34] M. G. B. Drew, V. Félix, I. S. Gonçalves, C. C. Romão, B. Royo, *Organometallics* **1998**, *17*, 5782–5788.
- [35] M. J. Calhorda, C. A. Gamelas, I. S. Gonçalves, E. Herdtweck, C. C. Romão, L. F. Veiros, *Organometallics* **1998**, *17*, 2597–2611.
- [36] S. S. Braga, I. S. Gonçalves, A. D. Lopes, M. Pillinger, J. Rocha, C. C. Romão, J. J. C. Teixeira-Dias, *J. Chem. Soc., Dalton Trans.* **2000**, 2964–2968.
- [37] J. R. Ascenso, I. S. Gonçalves, E. Herdtweck, C. C. Romão, *J. Organomet. Chem.* **1996**, *508*, 169–181.
- [38] R. Aguado, J. Escribano, M. R. Pedrosa, A. D. Cian, R. Sanz, F. J. Arnáiz, *Polyhedron* **2007**, *26*, 3842–3848.
- [39] V. S. Joshi, M. Nandi, H. Zhang, B. S. Haggerty, A. Sarkar, *Inorg. Chem.* **1993**, *32*, 1301–1303.
- [40] V. Cadierno, J. Díez, M. P. Gamasa, J. Gimeno, E. Lastra, *Coord. Chem. Rev.* **1999**, *147*, 193–195.
- [41] HA = angle between the medium planes subtended between planes (C1–C3) and (C1, C3, C8, C9); FA = angle between the medium planes subtended between planes (C1–C3) and (C4–C9); ΔM–C = 0.5 × (dM–C8 + dM–C9) – 0.5 × (dM–C1 + dM–C3).
- [42] a) A. C. Filippou, W. Grünleitner, E. Herdtweck, *J. Organomet. Chem.* **1989**, *373*, 325–342; b) C. J. Adams, K. M. Anderson,

- I. M. Bartlett, N. G. Connelly, A. G. Orpen, T. J. Paget, H. Phetmung, D. W. Smith, *J. Chem. Soc., Dalton Trans.* **2001**, 1284–1292; c) G. R. Willey, T. J. Woodman, M. G. B. Drew, *J. Organomet. Chem.* **1996**, *510*, 213–217.
- [43] D. K. Walanda, R. C. Burns, G. A. Lawrance, E. I. Von Nagy-Felsobuki, *J. Chem. Soc., Dalton Trans.* **1999**, 311–322.
- [44] L. Vilà-Nadal, E. F. Wilson, H. N. Miras, A. Rodríguez-Fortea, L. Cronin, J. M. Poblet, *Inorg. Chem.* **2011**, *50*, 7811–7819.
- [45] R. B. King, *Can. J. Chem.* **1969**, *47*, 559–568.
- [46] T. Kottke, D. Stalke, *J. Appl. Crystallogr.* **1993**, *26*, 615–619.
- [47] *APEX2 Data Collection Software, Version 2.1-RC13*, Bruker AXS, Delft, **2006**.
- [48] *Cryopad, Remote monitoring and control, Version 1.451*, Oxford Cryosystems, Oxford, **2006**.
- [49] *SAINTE+, Data Integration Engine, version 7.23a*, Bruker AXS, Madison, **1997–2005**.
- [50] G. M. Sheldrick, *SADABS, version 2.01*, Bruker AXS, Madison, **1998**.
- [51] a) G. M. Sheldrick, *SHELXS-97, Program for Crystal Structure Solution*, University of Göttingen, **1997**; b) G. M. Sheldrick, *Acta Crystallogr., Sect. A: Found. Crystallogr.* **2008**, *64*, 112–122.
- [52] G. M. Sheldrick, *SHELXL-97, Program for Crystal Structure Refinement*, University of Göttingen, Germany, **1997**.

Received: February 17, 2014
Published Online: July 7, 2014